Editors' Suggestion

First Measurement of Near-Threshold J/ψ Exclusive Photoproduction off the Proton

A. Ali,[10] M. Amaryan,[22] E. G. Anassontzis,[2] A. Austregesilo,[3] M. Baalouch,[22] F. Barbosa,[14] J. Barlow,[7] A. Barnes,[3] E. Barriga,[7] T. D. Beattie,[23] V. V. Berdnikov,[17] T. Black,[20] W. Boeglin,[6] M. Boer,[4] W. J. Briscoe,[8] T. Britton,[14] W. K. Brooks,[24] B. E. Cannon,[7] N. Cao,[11] E. Chudakov,[14] S. Cole,[1] O. Cortes,[8] V. Crede,[7] M. M. Dalton,[14] T. Daniels,[20] A. Deur,[14] S. Dobbs,[7] A. Dolgolenko,[13] R. Dotel,[6] M. Dugger,[1] R. Dzhygadlo,[10] H. Egiyan,[14] A. Ernst,[7] P. Eugenio,[7] C. Fanelli,[16] S. Fegan,[8] A. M. Foda,[23] J. Foote,[12] J. Frye,[12] S. Furletov,[14] L. Gan,[20] A. Gasparian,[19] V. Gauzshtein,[25,26] N. Gevorgyan,[27] C. Gleason,[12] K. Goetzen,[10] A. Goncalves,[7] V. S. Goryachev,[13] L. Guo,[6] H. Hakobyan,[24] A. Hamdi,[10] S. Han,[29] J. Hardin,[16] G. M. Huber,[23] A. Hurley,[28] D. G. Ireland,[9] M. M. Ito,[14] N. S. Jarvis,[3] R. T. Jones,[5] V. Kakoyan,[27] G. Kalicy,[4] M. Kamel,[6] C. Kourkoumelis,[2] S. Kuleshov,[24] I. Kuznetsov,[25,26] I. Larin,[15] D. Lawrence,[14] D. I. Lersch,[7] H. Li,[3] W. Li,[28] B. Liu,[11] K. Livingston,[9] G. J. Lolos,[23] V. Lyubovitskij,[25,26] D. Mack,[14] H. Marukyan,[27] V. Matveev,[13] M. McCaughan,[14] M. McCracken,[3] W. McGinley,[3] J. McIntyre,[5] C. A. Meyer,[3] R. Miskimen,[15] R. E. Mitchell,[12] F. Mokaya,[5] F. Nerling,[10] L. Ng,[7] A. I. Ostrovidov,[7] Z. Papandreou,[23] M. Patsyuk,[16] P. Pauli,[9] R. Pedroni,[19] L. Pentchev,[14,*] K. J. Peters,[10] W. Phelps,[8] E. Pooser,[14] N. Qin,[21] J. Reinhold,[6] B. G. Ritchie,[1] L. Robison,[21] D. Romanov,[17] C. Romero,[24] C. Salgado,[18] A. M. Schertz,[28] R. A. Schumacher,[3] J. Schwiening,[10] K. K. Seth,[21] X. Shen,[11] M. R. Shepherd,[12] E. S. Smith,[14] D. I. Sober,[4] A. Somov,[14] S. Somov,[17] O. Soto,[24] J. R. Stevens,[28] I. I. Strakovsky,[8] K. Suresh,[23] V. Tarasov,[13] S. Taylor,[14] A. Teymurazyan,[23] A. Thiel,[9] G. Vasileiadis,[2] D. Werthmüller,[9] T. Whitlatch,[14] N. Wickramaarachchi,[22] M. Williams,[16] T. Xiao,[21] Y. Yang,[16] J. Zarling,[12] Z. Zhang,[29] G. Zhao,[11] Q. Zhou,[11] X. Zhou,[29] and B. Zihlmann[14]

(GlueX Collaboration)

[1]*Arizona State University, Tempe, Arizona 85287, USA*
[2]*National and Kapodistrian University of Athens, 15771 Athens, Greece*
[3]*Carnegie Mellon University, Pittsburgh, Pennsylvania 15213, USA*
[4]*The Catholic University of America, Washington, D.C. 20064, USA*
[5]*University of Connecticut, Storrs, Connecticut 06269, USA*
[6]*Florida International University, Miami, Florida 33199, USA*
[7]*Florida State University, Tallahassee, Florida 32306, USA*
[8]*The George Washington University, Washington, D.C. 20052, USA*
[9]*University of Glasgow, Glasgow G12 8QQ, United Kingdom*
[10]*GSI Helmholtzzentrum für Schwerionenforschung GmbH, D-64291 Darmstadt, Germany*
[11]*Institute of High Energy Physics, Beijing 100049, People's Republic of China*
[12]*Indiana University, Bloomington, Indiana 47405, USA*
[13]*National Research Centre Kurchatov Institute, Institute for Theoretical and Experimental Physics, Moscow 117259, Russia*
[14]*Thomas Jefferson National Accelerator Facility, Newport News, Virginia 23606, USA*
[15]*University of Massachusetts, Amherst, Massachusetts 01003, USA*
[16]*Massachusetts Institute of Technology, Cambridge, Massachusetts 02139, USA*
[17]*National Research Nuclear University Moscow Engineering Physics Institute, Moscow 115409, Russia*
[18]*Norfolk State University, Norfolk, Virginia 23504, USA*
[19]*North Carolina A&T State University, Greensboro, North Carolina 27411, USA*
[20]*University of North Carolina at Wilmington, Wilmington, North Carolina 28403, USA*
[21]*Northwestern University, Evanston, Illinois 60208, USA*
[22]*Old Dominion University, Norfolk, Virginia 23529, USA*
[23]*University of Regina, Regina, Saskatchewan, Canada S4S 0A2*
[24]*Universidad Técnica Federico Santa María, Casilla 110-V Valparaíso, Chile*
[25]*Tomsk State University, 634050 Tomsk, Russia*
[26]*Tomsk Polytechnic University, 634050 Tomsk, Russia*
[27]*A.I. Alikhanian National Science Laboratory (Yerevan Physics Institute), 0036 Yerevan, Armenia*
[28]*College of William and Mary, Williamsburg, Virginia 23185, USA*
[29]*Wuhan University, Wuhan, Hubei 430072, People's Republic of China*

(Received 28 May 2019; revised manuscript received 5 July 2019; published 13 August 2019)

We report on the measurement of the $\gamma p \to J/\psi p$ cross section from $E_\gamma = 11.8$ GeV down to the threshold at 8.2 GeV using a tagged photon beam with the GlueX experiment. We find that the total cross

section falls toward the threshold less steeply than expected from two-gluon exchange models. The differential cross section $d\sigma/dt$ has an exponential slope of 1.67 ± 0.39 GeV^{-2} at 10.7 GeV average energy. The LHCb pentaquark candidates P_c^+ can be produced in the s channel of this reaction. We see no evidence for them and set model-dependent upper limits on their branching fractions $\mathcal{B}(P_c^+ \to J/\psi p)$ and cross sections $\sigma(\gamma p \to P_c^+) \times \mathcal{B}(P_c^+ \to J/\psi p)$.

DOI: 10.1103/PhysRevLett.123.072001

Introduction.—The exclusive production of charmonium near the threshold provides a unique probe for studying the gluonic field in the nucleon and its dynamical coupling to the valence quarks. Recently, there has been increased interest in J/ψ photoproduction in the beam energy region of $E_\gamma = 9.4$–10.1 GeV, as it can be used to search for the pentaquark candidates reported by LHCb in the $J/\psi p$ channel of the $\Lambda_b^0 \to J/\psi p K^-$ decay [1,2]. The LHCb Collaboration initially claimed two pentaquark states: $P_c^+(4380)$ and $P_c^+(4450)$ [1]. Very recently, they reported the observation of three narrow pentaquark states, $P_c^+(4312)$, $P_c^+(4440)$, and $P_c^+(4457)$, where the previously reported $P_c^+(4450)$ was resolved into the latter two states with narrower widths [2]. In photoproduction, these resonances can be produced in the s channel: $\gamma p \to P_c^+ \to J/\psi p$ [3–6], which is free from the three-body rescattering effects proposed as one of the possible explanations of the structures observed by LHCb [7–9]. This reaction can be described by the $P_c^+ \to J/\psi p$ decay plus its time inversion, with the $J/\psi - \gamma$ coupling determined by vector-meson dominance (VMD) [10]. The Breit-Wigner cross section depends on the measured width of the pentaquark, the VMD coupling obtained from the leptonic decay of the J/ψ, and only one unknown parameter, the branching fraction of the $P_c^+ \to J/\psi p$ decay that enters quadratically. The pentaquarks produced in the s channel would appear as structures in the J/ψ photoproduction cross section as a function of the beam energy, possibly interfering with the nonresonant continuum. By measuring the resonant contribution, one can estimate this branching fraction, which is complementary to the LHCb results.

A heavy quark system like the J/ψ interacts with the light quarks of the proton via gluon exchange. Close to the production threshold, a large momentum is transferred to the proton ($|t| = 2.2$ GeV^2 at the threshold). The energy dependence of the total cross section at high t has been addressed within several approaches. Based on dimensional scaling rules, the energy dependence of the J/ψ photoproduction cross section was predicted with a dependence on the number of hard gluons involved in the reaction [11]. Near the threshold, all valence quarks of the proton are expected to participate in the reaction, requiring the involvement of three high-x gluons, while at higher energies one or two hard gluons can be involved. In Ref. [12], it is argued that the t dependence of the exclusive reaction is defined by the proton gluonic form factor, for which a dipole form is assumed in analogy with the electromagnetic form factors:

$$F(t) \propto 1/(1 - t/m_0^2)^2, \tag{1}$$

though with a different mass scale m_0. The total cross section is proportional to the integral of $F^2(t)$ over a t range that, near the threshold, depends strongly on the beam energy. According to Ref. [13], J/ψ photoproduction near the threshold is dominated by the real part of the $J/\psi p$ elastic amplitude, which is of critical interest, since it contains the trace anomaly term related to the fraction of the nucleon mass arising from gluons. In Ref. [14], it was demonstrated that, in the near-threshold region, the shape of the cross section as a function of the energy and t depends on the contribution of gluons to the nucleon mass.

In this Letter, we report on the first measurement of the cross section of the exclusive reaction $\gamma p \to J/\psi p$ from the threshold up to $E_\gamma = 11.8$ GeV. We identify the J/ψ by its decay into an electron-positron pair. Previous measurements near the threshold were inclusive and done on nuclear targets. The only published result in our energy region is at $E_\gamma \approx 11$ GeV, measured at Cornell [15]. Measurements at SLAC have been performed at photon beam energies of 13 GeV and above [16].

The data were collected by the GlueX experiment located in Hall D at Jefferson Lab during 2016 and 2017, representing about 25% of the total data accumulated by the experiment to date.

The experiment.—The GlueX experiment uses a linearly polarized, tagged photon beam produced by the 12 GeV Continuous Electron Beam Accelerator Facility. The electron beam is incident on a diamond radiator and produces a bremsstrahlung spectrum proportional to $1/E_\gamma$ and a primary coherent peak adjusted to be in the energy range of 8.2–9.0 GeV. We also use data taken with an aluminum radiator, which does not produce coherent radiation. The scattered electron is analyzed with a 9 T m dipole magnet and detected in a tagging scintillator array allowing the photon energy to be determined with a resolution of 0.2%. The photon beam is collimated through a 5-mm-diameter hole at a distance of 75 m from the radiator. Following this, the photon flux and energy are monitored by an electron-positron pair spectrometer system [17].

The GlueX detector is based on a 2 T, 4-m-long solenoid magnet and has full azimuthal and $1° < \theta < 120°$ polar angle coverage. A 30-cm-long liquid hydrogen target is placed

inside the solenoid. A scintillating start counter surrounding the target helps to select the beam bunch [18]. Charged particle reconstruction around the target is performed by the central drift chamber (CDC), consisting of straw tubes grouped in 28 layers with axial and stereo orientation. In the forward direction, 24 planes of drift chambers with both wire and cathode strip readout are used [19]. The two drift chamber systems are surrounded by a lead-scintillator electromagnetic barrel calorimeter (BCAL) [20]. Electronically, the calorimeter is grouped in 192 azimuthal segments and in four radial layers, allowing the reconstruction of both transverse and longitudinal shower development.

The detector hermeticity in the forward direction outside of the magnet is achieved by the time-of-flight scintillator wall and the lead-glass electromagnetic forward calorimeter (FCAL), both located approximately 6 m from the target. Both calorimeters, FCAL and BCAL, are used to trigger the detector readout, requiring sufficient total energy deposition. The intensity of the beam in the region above the J/ψ threshold was 2×10^7 photons/s in 2016 and the first period of 2017 and was then increased to 5×10^7 photons/s for the rest of 2017, resulting in a total accumulated luminosity of $\sim 68\ \mathrm{pb}^{-1}$. In 2016, the maximum tagged photon energy was 11.85 GeV, while for 2017 it was lowered to 11.40 GeV. In 2017, the solenoid field was increased by 12% compared to 2016.

We study the exclusive reaction $\gamma p \to p e^+ e^-$ in the region of the e^+e^- invariant mass $M(e^+e^-) > 0.90$ GeV, which includes the narrow ϕ and J/ψ peaks, and the continuum dominated by the Bethe-Heitler (BH) process. Figure 1 shows the $M(e^+e^-)$ spectrum data after applying the event selection criteria described below. We normalize the J/ψ total cross section to that of BH in the invariant mass range 1.20–2.50 GeV, thus canceling uncertainties from factors like luminosity and common detector efficiencies.

The electron-pion separation is achieved mainly by applying selections on p/E, where the charged particle momentum p comes from the kinematic fit described below and E is the energy deposited in the calorimeters. We require $-3\sigma < p/E - \langle p/E \rangle < +2\sigma$ for both lepton candidates, where the resolution σ of p/E for the sample of leptons in the BH region is 3.9% for FCAL and 6.8% for BCAL. We also take advantage of the radial layer structure of the BCAL, using the energy deposited in the innermost layer, E_{pre}, and requiring lepton candidates emitted at a polar angle θ to have $E_{\mathrm{pre}} \sin\theta > 30$ MeV, taking into account the path length through the calorimeter. This rejects a significant number of pions, which deposit small amounts of energy in this layer compared to electrons. We require all charged particles to have momenta > 0.4 GeV and polar angle $> 2°$ in order to reduce the contamination from the $\pi^+\pi^- p$ final state and poorly reconstructed events. Because of the steeper t dependence of BH compared to $\pi^+\pi^-$ production, to minimize the pion background we select the BH process only in the low-t region, $-(t - t_{\mathrm{min}}) < 0.6\ \mathrm{GeV}^2$.

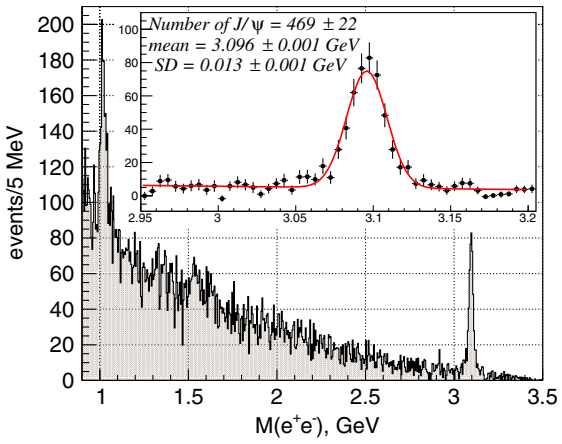

FIG. 1. Electron-positron invariant mass spectrum from the data. The inset shows the J/ψ region fitted with a linear polynomial plus a Gaussian (fit parameters shown).

Protons with momenta $\lesssim 1$ GeV are identified by their energy deposition in the CDC. The three final-state particles are required to be consistent in time with the same electron beam bunch (± 2 ns for most of the data). The tagged beam photons that are in time with this bunch qualify as possible candidates associated with the reaction. The contribution from beam photons accidental in time is subtracted statistically using a sample of photons that are out of time with respect to the reaction beam bunch.

Taking advantage of the exclusivity of the reaction and the relatively precise measurement of the beam energy, we use a kinematic fit to improve the resolution of the measured charged particle momenta. The fit enforces momentum and energy conservation and requires a common vertex for the three final-state particles. The electron-positron invariant mass spectrum in Fig. 1 is obtained using the results of the kinematic fit, which allows us to achieve a 13 MeV standard deviation (SD) mass resolution for the J/ψ. Studies of the kinematic fit show that the results are constrained primarily by the direction and magnitude of the proton momentum and the directions of the two leptons. In contrast to protons, the leptons are produced on average with higher momenta and smaller angles where the momenta are reconstructed with larger uncertainties. Therefore, they do not affect the kinematic fit noticeably.

We extract the J/ψ and BH yields in bins of beam energy or t. The J/ψ yield is obtained by performing a binned likelihood fit to the invariant mass spectra, as in Fig. 1, with a Gaussian signal and linear background.

The reduction of the background in the BH region by more than 3 orders of magnitude after applying the electron and positron selections event by event is not enough to completely eliminate the pion contamination. On average, the remaining sample contains 54% pions. To extract the BH yield, we fit the peak and the pion background of the p/E distribution for one of the lepton candidates, while

applying the p/E selection for the other candidate (see Supplemental Material [21]).

We have performed Monte Carlo simulations of both J/ψ and continuum BH production. The BH diagrams can be calculated in QED. We have used two BH generators, one based on analytical calculations [22] and another [23] based on numerical calculations of the diagrams. We generate the J/ψ-proton final state using an exponential t dependence and a cross section as a function of the beam energy obtained from our measurement, followed by the $J/\psi \to e^+e^-$ decay assuming helicity conservation.

The response of the GlueX detector to the generated events was simulated using GEANT3 [24]. Accidental tagger signals and detector noise signals were extracted from randomly triggered real data and injected into the generated events. We use these simulations to calculate the BH and J/ψ reconstruction efficiencies, $\varepsilon_{\rm BH}$ and $\varepsilon_{J/\psi}$. BH simulations are also used to integrate the BH cross section over the region used for normalization.

Results and discussion.—We calculate the total cross section in ten bins of beam energy using the following formula:

$$\sigma_{J/\psi}(E_\gamma) = \frac{N_{J/\psi}(E_\gamma)}{N_{\rm BH}(E_\gamma)} \frac{\sigma_{\rm BH}(E_\gamma)}{\mathcal{B}_{J/\psi}} \frac{\varepsilon_{\rm BH}(E_\gamma)}{\varepsilon_{J/\psi}(E_\gamma)}. \qquad (2)$$

Here $N_{J/\psi}$ and $N_{\rm BH}$ are the J/ψ and BH yields, respectively, $\sigma_{\rm BH}$ is the calculated BH cross section, and $\mathcal{B}_{J/\psi}$ is the $J/\psi \to e^+e^-$ branching ratio of 5.97% [25]. Note that the result depends on the relative BH to J/ψ efficiency. Effects due to variations in the photon flux over a given energy bin also cancel under the assumption that the J/ψ cross section varies slowly across a bin. The study of features in the J/ψ cross section that are narrower than an energy bin, such as those due to narrow pentaquarks, requires, in addition to the binned total cross sections, taking into account the finer flux structure.

We obtain results for the differential cross section in seven bins of t integrated over the region $E_\gamma = 10.00$–11.80 GeV. For the normalization of the differential cross section, we use the total BH yields instead of the yields in bins of t.

The total cross section in bins of beam energy and the differential cross section as a function of $-(t - t_{\rm min})$, together with the statistical and systematic errors, are given as Supplemental Material [21]. We estimate the overall normalization uncertainty to be 27%. The main contribution comes from the uncertainty in the relative BH to J/ψ efficiency determined from simulations, as the two processes occupy different kinematic regions. To test the accuracy of the simulations, we study the ratio of the measured BH cross section to the calculated one as a function of several kinematic variables, such as the proton momentum and polar angle. Comparing these ratios obtained for the BH and J/ψ kinematic regions, we find the largest relative difference to be $(23 \pm 18)\%$ and take the central value to be the uncertainty due to this source.

The radiative correction to the J/ψ decay is simulated using the PHOTOS package [26]. The results show that the kinematic fit recovers the J/ψ electron-positron invariant mass to its value before radiation. This is expected, because the dominant constraint to the fit is the recoil proton, which is decoupled from the J/ψ decay. This is not the case for the BH process, for which based on Ref. [27] we estimate 8.3% radiative correction in the extreme case, when the electron-positron invariant mass is not affected by the radiation, and only the proton is.

The maximum background contribution of the ρ' production to the e^+e^- continuum of 7% is estimated by comparing the results for two invariant mass ranges: 1.20–2.00 and 2.00–2.50 GeV. Based on Ref. [22], the contribution of timelike Compton scattering to the BH cross section is estimated to be less than 4%. Because of uncertainties of the generalized parton distribution model used in this estimation, we double this value as a systematic uncertainty.

We assign the systematic uncertainties of the individual data points to the maximum deviations of the results obtained by varying the procedures for fitting the J/ψ peak in the e^+e^- invariant mass spectrum and the BH electron and positron peaks in the p/E distribution. We assign the systematic error for the t slope to the maximum deviation of the slope obtained with different J/ψ fitting methods. The uncertainties of the parameters used in the J/ψ simulations (t slope and energy dependence) have a small effect.

As a cross-check, we have compared the total cross sections versus beam energy obtained from the 2016 and 2017 datasets, which represent different experimental conditions (solenoid field, photon beam intensity and spectrum). They are statistically consistent with an average ratio of 0.95 ± 0.14. Based on the missing mass distribution, we set a 5% upper limit for the target excitation contribution, $\gamma p \to J/\psi p \pi^0$.

For the t dependence of the differential cross section (see Supplemental Material [21]) for beam energies of 10.00–11.80 GeV with an average of 10.72 GeV, we obtain an exponential t slope of $1.67 \pm 0.35({\rm stat}) \pm 0.18({\rm syst})$ GeV^{-2}. This can be compared with the Cornell result at $E_\gamma \approx 11$ GeV of 1.25 ± 0.20 GeV^{-2} [15] and the SLAC result at $E_\gamma = 19$ GeV of 2.9 ± 0.3 GeV^{-2} [16]. All these results are consistent [28] with the hypothesis in Ref. [12] of the dipole t dependence for the differential cross section assuming a mass scale of 1.14 GeV, as given in Eq. (1).

The measured total cross section in bins of beam energy is shown in Fig. 2 and compared to the earlier measurements at Cornell [15] and SLAC [16]. Note that the SLAC experiment measured $d\sigma/dt$ at $t = t_{\rm min}$. In order to estimate the total cross section, we have integrated over t assuming the dipole t dependence with $m_0 = 1.14$ GeV.

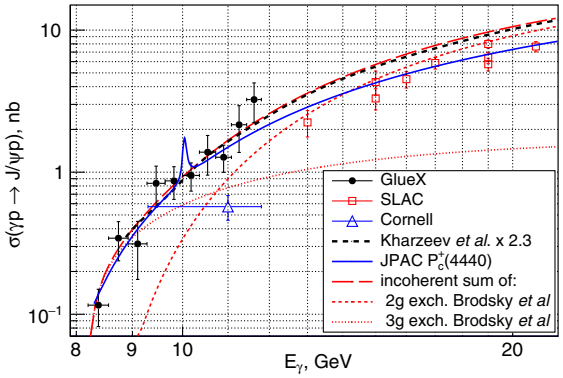

FIG. 2. J/ψ total cross section versus beam energy, compared to previous data [15,16], theoretical predictions [11,13], and the JPAC model [6] for $\mathcal{B}(P_c^+(4440) \to J/\psi p) = 1.6\%$ and $J^P = 3/2^-$. All curves are fitted or scaled to the GlueX data only. For our data, the quadratic sums of statistical and systematic errors are shown; the overall normalization uncertainty is 27%.

Comparing the J/ψ cross section to the Brodsky *et al.* model [11], we find that our data do not favor either pure two- or three-hard-gluon exchange separately, and a combination of the two processes is required to fit the data adequately. Such a combination is shown in Fig. 2, assuming no interference between the two contributions. It appears that three-hard-gluon exchange dominates near the threshold, consistent with the expectation that all the constituents should participate in the reaction.

The total cross-section calculations of Kharzeev *et al.* [13] imply a large gluonic contribution to the nuclear mass and are shown in Fig. 2 multiplied by a factor of 2.3. The shape of the curve agrees well with our measurements, and the overall scale factor is within the claimed uncertainty of the calculation.

The narrow LHCb states $P_c^+(4312)$, $P_c^+(4440)$, and $P_c^+(4457)$ produced in the s channel would appear as structures at $E_\gamma = 9.44$, 10.04, and 10.12 GeV, respectively, in the cross-section results shown in Fig. 2. We see no evidence for such structures. The initial report [1] claims the two states $P_c^+(4380)$ and $P_c^+(4450)$ may have spin $3/2$ or $5/2$ with opposite parity. The spins and parities of the new states $P_c^+(4312)$, $P_c^+(4440)$, and $P_c^+(4457)$ have not been determined yet. We evaluate the branching fraction limits $\mathcal{B}(P_c^+ \to J/\psi p)$ individually for each P_c assuming $J^P = 3/2^-$, with the lowest angular momentum $L = 0$ of the $J/\psi p$ system. As VMD leads to an increase in the cross section for increasing L [4], $L = 0$ minimizes the resulting cross section and, therefore, yields a maximal upper limit on the branching fraction. We fit our data, in which the statistical and systematic uncertainties on the individual points are added in quadrature, with a variation of the Joint Physics Analysis Center (JPAC) model [6], where the nonresonant component is described by a combination of Pomeron and tensor amplitudes [29]. To take into account the fine flux variations (see Supplemental Material [21]), in each bin the data are fitted with the integral of the model function weighted by the normalized flux distribution across the extent of the bin. The upper limits on the branching fractions are determined by integrating the profile likelihood of the fit as a function of the branching fraction. The profile likelihood is determined by a procedure based on the one described in Ref. [30], in which uncertainties on the model parameters can be incorporated. As an example of the sensitivity of our measurement, we plot in Fig. 2 the model prediction for $P_c^+(4440)$ with $\mathcal{B}(P_c^+(4440) \to J/\psi p) = 1.6\%$, which is the estimated upper limit at 90% confidence level when taking into account the errors of the individual data points only. Similar curves for the other resonances are shown in Supplemental Material [21]. Including systematic uncertainties due to the nonresonant parametrization, Breit-Wigner parameters, and overall cross-section normalization, we determine upper limits at 90% confidence level of 4.6%, 2.3%, and 3.8% for $P_c^+(4312)$, $P_c^+(4440)$, and $P_c^+(4457)$, respectively. These upper limits become a factor of 5 smaller if $J^P = 5/2^+$ is assumed. Note that these results depend on the interference between the pentaquarks and the nonresonant continuum that is model dependent and the interference between the pentaquarks that is not taken into account.

A less model-dependent limit is found for the product of the cross section at the resonance maximum and the branching fraction, $\sigma_{\max}(\gamma p \to P_c^+) \times \mathcal{B}(P_c^+ \to J/\psi p)$, using an incoherent sum of a Breit-Wigner function and the nonresonant component of the model described above. Applying the same likelihood procedure that includes the systematic uncertainties yields upper limits at 90% confidence level of 4.6, 1.8, and 3.9 nb for $P_c^+(4312)$, $P_c^+(4440)$, and $P_c^+(4457)$, respectively.

In Refs. [31–33], the partial widths of the $P_c^+ \to J/\psi p$ decays were calculated and shown to be orders of magnitude different for two pentaquark models, the hadrocharmonium and molecular models. Our upper limits on the branching fractions do not exclude the molecular model but are an order of magnitude lower than the predictions in the hadrocharmonium scenario.

In summary, we have made the first measurement of the J/ψ exclusive photoproduction cross section from $E_\gamma = 11.8$ GeV down to the threshold, which provides important inputs to models of the gluonic structure of the proton at high x. The measured cross section is used to set model-dependent upper limits on the branching fraction of the LHCb P_c^+ states, which allow us to discriminate between different pentaquark models.

We acknowledge the outstanding efforts of the staff of the Accelerator and the Physics Divisions at Jefferson Lab that made the experiment possible. This work was supported in part by the U.S. Department of Energy, the U.S. National Science Foundation, the German Research Foundation, GSI Helmholtzzentrum

für Schwerionenforschung GmbH, the Natural Sciences and Engineering Research Council of Canada, the Russian Foundation for Basic Research, the United Kingdom Science and Technology Facilities Council, the Chilean Comisión Nacional de Investigación Científica y Tecnológica, the National Natural Science Foundation of China, and the China Scholarship Council. This material is based upon work supported by the U.S. Department of Energy, Office of Science, Office of Nuclear Physics under Contract No. DE-AC05-06OR23177. S. D. acknowledges the support of Jefferson Science Associates, LLC.

*Corresponding author.
pentchev@jlab.org

[1] R. Aaij *et al.* (LHCb Collaboration), Phys. Rev. Lett. **115**, 072001 (2015).
[2] R. Aaij *et al.* (LHCb Collaboration), Phys. Rev. Lett. **122**, 222001 (2019).
[3] Q. Wang, X.-H. Liu, and Q. Zhao, Phys. Rev. D **92**, 034022 (2015).
[4] V. Kubarovsky and M. B. Voloshin, Phys. Rev. D **92**, 031502(R) (2015).
[5] M. Karliner and J. Rosner, Phys. Lett. B **752**, 329 (2016).
[6] A. N. Hiller Blin, C. Fernandez-Ramirez, A. Jackura, V. Mathieu, V. I. Mokeev, A. Pilloni, and A. P. Szczepaniak, Phys. Rev. D **94**, 034002 (2016).
[7] F.-K. Guo, U.-G. Meißner, W. Wang, and Z. Yang, Phys. Rev. D **92**, 071502(R) (2015).
[8] X. H. Liu, Q. Wang, and Q. Zhao, Phys. Lett. B **757**, 231 (2016).
[9] M. Mikhasenko, arXiv:1507.06552.
[10] The possible limitations of the VMD for heavy quark mesons are discussed in Ref. [4].
[11] S. Brodsky, E. Chudakov, P. Hoyer, and J. Laget, Phys. Lett. B **498**, 23 (2001).
[12] L. Frankfurt and M. Strikman, Phys. Rev. D **66**, 031502(R) (2002).
[13] D. Kharzeev, H. Satz, A. Syamtomov, and G. Zinovev, Nucl. Phys. **A661**, 568 (1999).
[14] Y. Hatta and D.-L. Yang, Phys. Rev. D **98**, 074003 (2018).
[15] B. Gittelman, K. M. Hanson, D. Larson, E. Loh, A. Silverman, and G. Theodosiou, Phys. Rev. Lett. **35**, 1616 (1975).
[16] U. Camerini, J. Learned, R. Prepost, C. Spencer, D. Wiser, W. Ash, R. L. Anderson, D. M. Ritson, D. Sherden, and C. K. Sinclair, Phys. Rev. Lett. **35**, 483 (1975).
[17] F. Barbosa, C. Hutton, A. Sitnikov, A. Somov, S. Somov, and I. Tolstukhin, Nucl. Instrum. Methods Phys. Res., Sect. A **795**, 376 (2015).
[18] E. Pooser, F. Barbosa, W. Boeglin, C. Hutton, M. Ito, M. Kamel, P. K. A. LLodra, N. Sandoval, S. Taylor, T. Whitlatch, S. Worthington, C. Yero, and B. Zihlmann, Nucl. Instrum. Methods Phys. Res., Sect. A **927**, 330 (2019).
[19] L. Pentchev, F. Barbosa, V. Berdnikov, D. Butler, S. Furletov, L. Robison, and B. Zihlmann, Nucl. Instrum. Methods Phys. Res., Sect. A **845**, 281 (2017).
[20] T. D. Beattie, A. M. Foda, C. L. Henschel, S. Katsaganis, S. T. Krueger, G. J. Lolos, Z. Papandreou *et al.*, Nucl. Instrum. Methods Phys. Res., Sect. A **896**, 24 (2018).
[21] See Supplemental Material at http://link.aps.org/supplemental/10.1103/PhysRevLett.123.072001 for numerical results and additional plots.
[22] E. Berger, M. Diehl, and B. Pire, Eur. Phys. J. C **23**, 675 (2002).
[23] R. Jones, Numerical calculations of the tree level QED diagrams using Diracxx package, https://github.com/rjones30/Diracxx.
[24] R. Brun *et al.*, Report No. CERN-DD-78-2-REV, 1978.
[25] M. Tanabashi *et al.*, Phys. Rev. D **98**, 030001 (2018).
[26] E. Barberio, and Z. Wąs, Comput. Phys. Commun. **79**, 291 (1994).
[27] M. Heller, O. Tomalak, and M. Vanderhaeghen, Phys. Rev. D **97**, 076012 (2018).
[28] L. Pentchev (for the GlueX Collaboration), in Proceedings of the 8th International Conference on Quarks and Nuclear Physics (to be published).
[29] V. Mathieu (private communication).
[30] W. A. Rolke, A. M. Lopez, and J. Conrad, Nucl. Instrum. Methods Phys. Res., Sect. A **551**, 493 (2005).
[31] M. I. Eides, V. Yu. Petrov, and M. V. Polyakov, Eur. Phys. J. C **78**, 36 (2018).
[32] M. I. Eides and V. Yu. Petrov, Phys. Rev. D **98**, 114037 (2018).
[33] M. I. Eides, V. Y. Petrov, and M. V. Polyakov, arXiv:1904.11616.